DOKUZ EYLÜL UNIVERSITY

GRADUATE SCHOOL OF NATURAL AND APPLIED SCIENCES

CRACK INSPECTION USING IMAGE PROCESSING

by

Çağatay GÖNCÜ

October, 2019

İZMİR

CRACK INSPECTION USING IMAGE PROCESSING

A Thesis Submitted to the
Graduate School of Natural and Applied Sciences Dokuz Eylül University
In Partial Fullfilment of the Requirements for the Degree of Master of Science
in Electrical and Electronics Engineering

by
Çağatay GÖNCÜ

October, 2019
İZMİR

M.Sc THESIS EXAMINATION RESULT FORM

We have read the thesis entitled **"CRACK INSPECTION USING IMAGE PROCESSING"** completed by **ÇAĞATAY GÖNCÜ** under supervision of **ASSIST. PROF. DR. YAVUZ ŞENOL** and we certify that in our opinion it is fully adequate, in scope and in quality, as a thesis for the degree of Master of Science.

Assist. Prof. Dr. Yavuz ŞENOL

Supervisor

Prof. Dr. Mehmet Engin

(Jury Member)

Assist. Prof. Dr. Hakkı T. YALAZAN

(Jury Member)

Prof.Dr. Kadriye ERTEKİN

Director

Graduate School of Natural and Applied Sciences

ACKNOWLEDGEMENTS

First of all, I would like to express my deepest gratitude to project advisor Assist. Prof. Dr. Yavuz ŞENOL for continuous guidance, generous. I am grateful for your guidance throughout my graduate education.

In addition, I thank my company TUBITAK for their support. Ph. D. Etem DENİZ, for precious thoughts that enhance the performance of the project.

At last, I would like to thank my family and my wife Hazal OLUK GÖNCÜ for their trust, patience and encouragement.

Çağatay GÖNCÜ

CRACK INSPECTION USING IMAGE PROCESSING

ABSTRACT

Cracks can damage the concrete's structure. Large structural problems can occur in concrete structures when the cracks expand. Crack detection can avoid the main problems. This project puts forward a new technique of crack detection in the processing of images.

The proposed crack detection method generally consists of four steps. Converting input image to a gray-scale image and then using Gauss Filter and Median Filter for removing noise from a gray-scale image is first step. Secondly, the gradient of the first step output image is determined and the maximum non-suppression is applied to the gradient image and then mapped for noise removal. Thirdly; the binary image is obtained from the second step output image and the binary image is applied with a morphological close operation. In the fourth, the crack detection threshold is calculated to decide whether the image input has a crack or not. For two hundred concrete sample images with one hundred non-crack and one hundred crack images, the accuracy of the proposed method is equal to ninety-six percent. You can accept this method that the images are not cracks or cracks. This method can be used to find sample images have cracks or not.

Keywords: Crack detection, image processing, concrete structure

GÖRÜNTÜ İŞLEME İLE ÇATLAK İNCELEMESİ

ÖZ

Çatlaklar betonun yapısına zarar verebilir. Beton yapılardaki çatlaklar genişlediğinde büyük yapısal problemler ortaya çıkabilir. Çatlak tespiti kullanımı ana problemleri önleyebilir. Bu makale görüntülerin işlenmesi için yeni bir çatlak algılama yöntemi sunar.

Önerilen yöntem genel olarak 4 adımdan oluşmaktadır: ilk; giriş görüntüsünü gri tonlamalı bir görüntüye dönüştürme ve ardından gri tonlamalı bir görüntüden paraziti gidermek için Gauss Filtresi ve Medyan Filtresi kullanılmıştır. İkinci; İlk adım, çıktı görüntüsünün gradyanı ile belirlenir ve maksimum sıkıştırma olmayan gradyan görüntüsüne uygulanır ve daha sonra gürültüyü gidermek için eşlenir. Üçüncü; İkinci adım çıktı görüntüsü, ikili bir resme dönüştürülür ve ikili görüntü, morfolojik bir closing işlemle uygulanır. Dördüncü; çatlak algılama eşiği hesaplanır ve görüntü girişi çatlak mı yoksa çatlak değil mi olduğu belirlenir. Yüz çatlak olamayan ve yüz çatlak görüntü içeren iki yüz somut örnek görüntü için, önerilen yöntemin doğruluğu yüzde doksan altıya eşittir. Bu yöntem, görüntülerin çatlak veya çatlak olmadığını ayırt edebilmektedir.

Anahtar Kelimeler: Çatlak tespiti, görüntü işleme, beton yapı

CONTENTS

LIST OF FIGURES

Page

LIST OF TABLES

Page

CHAPTER ONE
INTRODUCTION

The concrete structures could have concrete cracking. Crack inspection is very substantial for the life of the structure. Concrete cracks affect the view of the surface, load carrying capacity, and its strength. Hence, crack inspection is very important. Generally, traditional visual inspection method performed by experts is used to investigate cracks. However, that is a subjective method and the performance of the examination heavily depends on the crack inspector, and therefore, the inspection results changes day by day. In this regard, development of new efficient methods is necessary to obtain good information of cracks (Nishikawa, Yoshida, Sugiyama, & Fujino, 2012).

The concrete cracks can be found in poured concrete structures vertically, horizontally or diagonally. The Figure 1.1 is an example of concrete structure crack.

Figure 1.1 Crack sample image (Ozgenel, 2018)

1.1 Literature Review

Several methods have been used in image processing algorithms for detection of concrete surface cracks. There is a study which compares four methods which are Fast Fourier and Fast Haar transforms, Sobel and Canny operators. This work shows Fast Haar transform is more effective than other methods (Abdel-Qader, Abudayyeh, & Kelly, 2003).

Multiple filtering and Otsu threshold methods used to detect cracks is described in (Talab, Huang, Xi, & HaiMing, 2016). There are three steps in Talab's method. Firstly, the image is converted to gray-scale formatted image and Sobel's filter is used to detect cracks. Secondly, suitable thresholded binary image is used to separate foreground and background of the image. Finally, noise in the image is reduced using Sobel's filter and the cracks are detected using Otsu's method.

For detection of small cracks in concrete structures, an image processing algorithm was presented by (Yang, Yang, & Huang, 2015). In their research, two cameras were used to take photos and then the image analysis procedures were applied on these photos. This procedure included the following major processing steps. These steps were calibration of stereo, control focuses situating, prediction for surface equation, metric adjustment, corruption examination, and scanning.

Lins and Givigi present a method to estimate crack dimension. Hue, saturation and value color range of red, green, blue color space were used in the crack detection algorithm. The algorithm detects the cracks and marks the crack locations. The crack dimensions are estimated using pixel positions and numbers of pixels within the neighbor of defined cracks (Lins & Givigi, 2016).

Qingbo, in his study, improved the algorithm of crack image processing which consists of image enrichment, median filtering and converting gray level. The result of algorithm based on image segmentation and crack detection showed that this study removes noise, concretizes the margin and improves the segmentation precision (Qingbo, 2016).

Shen identifies the category of cracks on pavements. In different crack conditions, which are transverse, longitudinal, and turtle surface images were collected. After collection process, gray transform is applied to the surface images. In the final step, in order to identify crack category, mathematical morphology operation performed to the images. Choosing the pavement examples to test, the outcomes demonstrate that this distinguishing proof calculation could precisely distinguish the classification of split (Shen, 2016).

Qi and his friends propose an algorithm based on image processing for crack detection. Their method, which has block binarization, facilitates the image processing sequence. According to the differences between the noise and cracks on images, noisy pixels are taken away. At long last, crack detection can be distinguished consequently (Qi, Liu, Wu, & Zhang, 2014).

Xuhang Tong and his friends propose a machine vision system with using image processing to exam cracks on the concrete bridges in real time The efficiency of result shows that this method is greater than the Canny method and Fujita's method (Xuhang Tong, Jie Guo, Yun Ling, & Zhouping Yin, 2011).

Maode and his friends aim to provide both fast and effective image processing technique on high-grade highway. In order to make balance, they introduce the morphology to crack inspection on pavement and present a new image processing technique. Four structural elements are used to create a median filtering algorithm to have enhanced the gray-level pavement images. To take out edges from the gray-level pavement image, morphological close and morphological gradient operations are applied together. The morphology-erosion operator is applied to the image to enhance thin cracks and obtain the skeletons. So, total length of each skeleton indicates the crack lengths. In this way, this method could precisely determine crack length and crack width (Maode, Shaobo, Kun, & Yuyao, 2007).

A binarization threshold is used to detect crack pixels in the image. Instead of traditional median filter a block filter technique is used to remove noises. The better results are obtained by using block filter technique. After eliminating the noises from the image, morphological operations are performed to obtain crack sketch (Huayong Wu, Rongxin Zhao, & Bo Li, 2011).

Zhaoyun and his friends propose a method which characterizes the crack types and indicates the crack properties which are its length and its width. The sample images are procured by camera in this project. The cracks on the pavement surface are processed and classified into groups which are line and alligator cracks according to topological properties. At that point the line cracking group could be longitudinal or transverse (Zhaoyun, Chaofan, & Aimin, 2009).

The crack inspection algorithm with using image pre-processing is mentioned in this project (Li & Wang, 2015). The Graying arithmetic method, image denoising method and image enhancement are parts of the image pre-processing method. According to this paper, the crack extraction algorithm can be obtained by two ways. One of them is image edge detection. The image edge detection method can be performed by using Robert, Prewitt, Laplacian, Canny and Sobel edge detection operators. The other method of the crack extraction algorithm is Mathematical Morphological Image Processing. Dilation, erosion, opening and closing operators are basic morphological operators. The wavelet transform can be used for crack extraction. The Heuristic edge connection method and Region-growing Crack Connection arithmetic are the common crack detection methods.

There is a new approach based on continuous Wavelet transform for crack identification on pavement surface images. The first step is the application of wavelet transform and creation of the complex coefficient maps. In addition, the information about modulus and angle is utilized to hold important parameters. At that point, the maximum values of wavelet parameters are determined. At last, the information which has cracks is obtained by having a binary image (Subirats, Dumoulin, Legeay, & Barba, 2006).

To improve driving functions under non-smooth roads, a road crack detection method is proposed by (Premachandra, Waruna, Premachandra, & Parape, 2013). To start with, the road surfaces which incorporate crack pixels are extricated as crack images in regards to the pixel fluctuation of the road image. At last cracks are detected on sample images. As per tests, new proposition indicated better execution contrasted with the traditional techniques.

Four methods, which are combined technique, morphological operation, infiltration method, and applied method for the crack inspection, are mentioned in this study (Wang & Huang, 2010). The first three methods are crack inspection method automatically except applied method. Because applied method is semi-automatic. The combined technique is convenient for pretreatment but performance of combined technique is hinge on parameter of its filter. Although some cracks are not detected exactly, the performance of morphological operation is better than Otsu's method. Infiltration method is good for uncertain surfaces, because this technique is regional. Consequently, applied method gives the best performance for crack inspection.

Amhaz and Chambon and their friends propose a review of existing method on the basis of choosing of least ways for pavement crack detection. They present an improved variant of a calculation dependent on insignificant way choice by diminishing loop and spike ancient rarities in the crack detection. Consequently, Minimal Path Selection can detect cracks with variable extents throughout the framework of any form (Amhaz, Chambon, Idier, & Baltazart, 2014).

To detect cracks on the surface Adaptive Canny Algorithm and threshold technique are performed (Qiang, Guoying, Jingqi, & Hongmei, 2016). Initially, the spatial scale factor of Gaussian filter is determined by using intensity of existing pixel and average intensity of all pixels. In the second step, to get threshold values which are high and low Otsu threshold technique is performed to get image gradient. To get edge inspection on the crack image two threshold values are utilized. At last, using threshold technique cracks on the image are obtained. According to outcomes, the edges of crack can be obtained with this technique.

The image processing toolbox with using image processing algorithms to get crack inspection on the asphalt surfaces are presented by (Oliveira & Correia, 2014). This toolbox consists of pre-processing algorithms, crack detection and characterization algorithms, and accuracy assessment techniques. The image database is created on road, which is uncommon examination with 84 pavement images. The yields with using images from database show the potential of the techniques.

Hu and his friends propose a novel method to obtain the features of the samples. To recognition and localization for cracks on the wall, the linear feature of the digital image is extracted from the image. Using the maximum and the minimum gray value of the level image, dynamic threshold value is calculated. The non-cracked edges can be removed with utilizing Prewitt technique and the edge data remains all the more precisely. After edge detection process, isolated points are removed. In light of the straight development highlight of cracks, expelling anomalies can make the extraction and investigation of cracks increasingly helpful and compelling. Through the former steps, there is lots of linear information. To remove the cracks from edges on the image, the edge set is decomposed into segments. The polynomial fitting method is performed to each segments and parameter analysis is applied. At the last, cracks are marked (Hu, Tian, Yang, Xu, & Wang, 2012).

A real-time technique to get crack inspection is shown by (Sy, Avila, Begot, & Bardet, 2008). The image projection, the morphological processing, and thresholding technique are used in this study. There are three image types to analyze the performance of method. These types are optimal and random lightning environments, and images obtained from the machine. Hereby, the performance of method is suitable for crack inspection.

Oliveira and Correia show another technique to distinguish crack from image caught amid surface reviews, notwithstanding as these cracks show up confusing form. There are two phases in the surface crack inspection method: (i) choice of noticeable "crack seeds", embracing a productive segmentation processing, limiting the discovery of results which are false positives, after suitable image smoothing; (ii) to distinguish the crack forms which are non-crack or crack, binary pixel sorting process is performed. To analyze that the crack classification is suitable or not for the crack inspection. At last, the cracks are classified into groups that are transversal or longitudinal (Oliveira & Correia, 2017).

A system which inspects the pavement surface images is created by (Oliveira & Correia, 2008). These images were obtained from roads in Portugal. The system detects cracks or non-cracks field with using non-overlapping grids which obtains black-white form of the image with clearing non-crack pixels from the image to classify cracks into groups that are transversal and longitudinal. The results of the system assert incentive inspections for detection with automatically.

A novel system to clear and inspect cracks on the images is proposed by (Giakoumis, Nikolaidis, & Pitas, 2006). To detect cracks on the images, morphological top-hat transform and thresholding is performed. This system provides semi-automatic removing false-positive cracks on the images with using neural network. At last, cracks are filled based on filters and this study shows us an advance methodology for the removing cracks from the images.

There is a novel unmanned crack inspection system on the two-dimension gray level pavement images. This system is provided with Otsu thresholding technique. There are three steps for the inspection. In the initial step, four images are determined from the sample images. On the four images, the threshold is used to investigate cracks. This threshold is determined by using Otsu threshold method and histogram for the four images. Hence, the system provides inspection very fast and low SNR (signal-to-noise ratio) value (Akagic, Buza, Omanovic, & Karabegovic, 2018).

To obtain crack inspection automatically and save costs for the supervisors a novel method is recommended (Mancini, Malinverni, Frontoni, & Zingaretti, 2013). Gradient Vector Flow method classifies cracks precisely fit curve with using extraction of features from the images. Another method is fuzzy logic technique based on the pixel intensities and pixel neighbors. The cracks are formed of the darkest pixels in the pavement images. So, the information about the surface is obtained with this system to control the repairment of the surfaces.

To utilize crack inspection, the geometrical features of the surface obtained from a van with three-dimension camera were used by (Zalama, Gómez-García-Bermejo, Medina, & Llamas, 2014). The main assistant of the system is acquiring features. When transversal cracks exist, laser lightning is blocked. Two and three dimension techniques acquire precision of 96.6% for transverse cracks. In addition, for longitudinal cracks precision is equal to 93.3%. When these two results are compared with the study in (Medina-Carnicer, Madrid-Cuevas, Carmona-Poyato, & Muñoz-Salinas, 2009), it is seen that the results are improved.

Zhang and his friends present a novel method to crack detection. They use an algorithm based on training of each image to classify with supervised deep convolutional neural network. Five hundred images, gathered with a cell, are used to evaluate algorithm. When prevalent existing hand-created techniques are compared with crack detection execution, the new system is better than the old one (Zhang, Yang, Daniel Zhang, & Zhu, 2016).

Choudhary and Dey presented neural network and fuzzy logic and image processing for crack detection in concrete surfaces. In the system, the cracks inspection techniques with image processing are used to obtain properties from pavement images. Two sorts of methodologies have been executed in this investigation: the image processing which groups an image in general, and the item approach, which arranges every segment or article in an image into cracks and noise. The models have been tried on 205 images and assessed based on five proportions of execution (Choudhary & Dey, 2012).

Xu, Ma, and their friends present a novel crack inspection technique with using Back Propagation (BP) neural network. Histogram equalization method, spatial filtering, and binary processing are applied in image pre-processing technique. The pavement surface structure is afterwards separated to small image. The learning samples are extracted from each small image. These samples are used to train BP neural network. At last BP neural network arrange yields to compose connection of cracks for better distinguishing proof exactness. The experiments informs that BP neural network provides the recognition of the cracks accurately (Xu, Ma, Liu, & Niu, 2008).

1.2 The Outline of the Thesis

This project consists of four chapters, which are introduction, proposed crack detection method, conclusion part and reference. In the primary section, the inspiration driving this proposition is examined and postulation targets are characterized. Additionally, concise data is given about foundation and cases of past works are quickly mentioned. In the second part, method for working and philosophy is characterized. In light of indicated arrangement, plan and execution are detailed. In the third part, results are assessed and contrasted and comparable plans. Likewise, conceivable future improvement is discussed. In the last part, all connected assets incorporate books, diaries; advanced documents and so forth are referred to.

CHAPTER TWO
BACKGROUND

In this chapter, the explanation of the technical methods is given for the proposed threshold method. These technical methods are; converting from RGB image to gray-scale image, Gaussian smoothing, median filtering, Sobel operation, non-maximum suppression, morphological close operation hysteresis thresholding, a brief explanation of the neural network.

2.1 Converting RGB Image to Gray-scale Image

The example image or color map in red-green-blue color space (R(x,y), G(x,y), and B(x,y)) is converted to gray scale intensity image, I(x,y), is mentioned in equation 2.1.

$$I(x,y) = 0.298936 * R(x,y) + 0.587043 * G(x,) + 0.114021 * B(x,y) \qquad (2.1)$$

2.2 Gaussian Smoothing

Gaussian Smoothing (Gaussian blur) is used to apply smoothing on a given image. This method is commonly used in graphics software especially to reduce noise in the image. It is also used in pre-processing algorithms of the computer vision algorithms. Gaussian blur is, mathematically, identical to convolution of the image processed by Gaussian function. Gaussian function in two-dimension is represented with equation 2.2.

$$G(x,y) = \frac{1}{2\pi\sigma^2} * \ e^{-\frac{x^2+y^2}{2\sigma^2}} \qquad (2.2)$$

where x is the remove from the root on the horizontal hub and y is the remove from the root on the vertical hub and σ is the standard deviation of the Gaussian distribution. Gaussian blur method preserves boundaries and edges as shown in Figure 2.1.

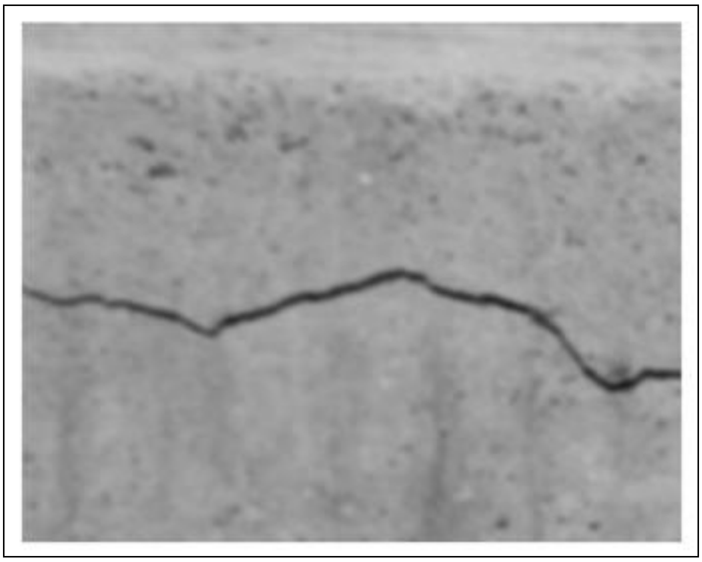

Figure 2.1 The image by Gaussian blurred for Figure 1.1

2.3 Median Filtering

The Median Filter is generally used for noise removing from an image in a non-linear way. To do this, each pixel within the image is evaluated together with all adjacent neighboring pixels, which all together can be named a frame, to find the correct representative for the centered pixel. All the values in the frame are sorted to find the median value, and then the center value is replaced with the median one. All image pixels in the middle of a frame are replaced by the median of all frame values. To cover complete image the window is slide pixel by pixel. After handling the Gaussian filter on the excellent picture of Figure 1.1. The median filter is performed and is appeared in Figure 2.2. This show the effect of noise removing without affecting the borders within the image.

Neighborhoods values of the matrix M is 115;119;120;123;124;125;126;127;150 for 3x3 square neighborhood, respectively. The median value of this matrix is 124.

$$M = \begin{pmatrix} 150 & 125 & 126 \\ 127 & 115 & 119 \\ 124 & 123 & 120 \end{pmatrix}$$

Figure 2.2 The result of median filter processing of sample image in Figure 1.1

2.4 Sobel Operator

Sobel operator which is also known as Sobel filter is utilized in computer vision especially within edge detection processing where it highlights edges in an image. The gradient of image intensity function is determined by Sobel operator. This processing convolves the image with horizontal and vertical directions based on two 3x3 kernels which are shown in Figure 2.3. At the end of Sobel filter processing the edges of the image is strengthened.

$$G_x = \begin{pmatrix} -1 & 0 & +1 \\ -2 & 0 & +2 \\ -1 & 0 & +1 \end{pmatrix} \qquad G_y = \begin{pmatrix} -1 & -2 & -1 \\ 0 & 0 & 0 \\ +1 & +2 & +1 \end{pmatrix} \tag{2.3}$$

$$G = \sqrt{(G_x)^2 + (G_y)^2} \qquad \Theta = \arctan\left({}^{G_y}\!/_{G_x}\right) \tag{2.4}$$

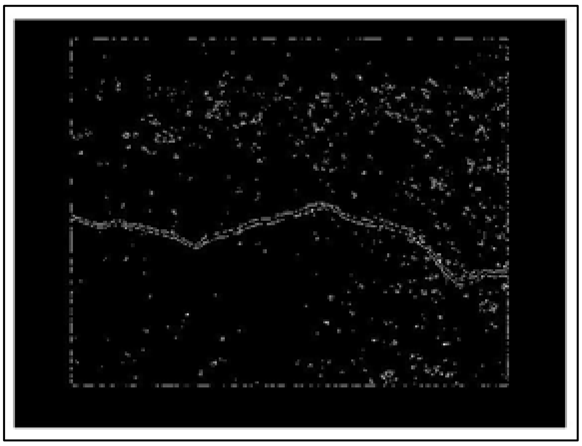

Figure 2.3 Sobel operator performed image of sample image in Figure 1.1

2.5 Non-Maxima Suppression Technique

Non-maximum suppression technique is essential part of the image processing utilized in computer vision such as many edge, corner or object detection algorithms, (Rothe, Guillaumin, & Van Gool, 2015).

The objective of non-maxima suppression will be locating the genuine local areas and stifling the others. When searching objects in an image a few are generally found as points however some of them are not by any stretch of the imagination objects. Non-Maxima Suppression (NMS) comprises in select which of those maxima's are truly questions and stifle those that are definitely not. NMS algorithm consists of following steps; find the maxima, interpolate to know how big the bounding box should be, create the bounding box, and clear the maxima point and nearly pixels.

2.5.1 Find the Maxima

At this part of the non-maxima suppression, the highest value of every sub-images are found and putting away the value and the position in different vectors with length.

Figure 2.4 Dilate operation performed image of sample image in Figure 1.1

2.5.2 Interpolation

Depending on which sub-image has the highest value, the bouncing box will have an alternate size to fit the item as precisely as could reasonably be expected. To do this the algorithm introduces the two most elevated qualities got in the past advance, those qualities speak to which images are closer to the size of the item and considering the two qualities with the known scales an exact size for the object can be induced.

2.5.3 Creation of the Bounding Box

When the size of the item is realized the jumping box can be fabricated. Being known the center of the item (maxima) what the algorithm does is discovering two sides of the bouncing box, the upper left corner and the base right corner. The program has put away the separation between the center of the item and the diverse corners for an object of a scale 100%, increasing this incentive by the scale got in the past advance we can acquire the situation of the distinctive corners.

Figure 2.5 Erode operation illustrates the result image for the image in Figure 1.1

2.5.4 Removing the Maxima Point

When the bouncing box is made the algorithm proceeds to remove the maxima that made it and its environment. This is finished by presenting a square shape of zeros in the sub-images. Depending in which of the sub-images were the maxima the square shape will be greater or littler, greater if is a major scale and little if it's a little one.

2.6 Morphological Close Operation

The morphological close operation is combination of the morphological dilation and erosion operations. The morphological dilation operation that can be shown in Figure 2.4 makes objects increasingly noticeable and fills in little gaps in objects. This can be done by selecting a pixel in the image and setting the value of pixel in respect to the neighboring pixel value. The selected pixel can be set to 1, if any of the neighboring pixels is set to 1. This can make pixels more noticeable by increasing the connectivity within the neighboring pixels. The morphological erosion operation is opposite of the morphological dilation operation is shown in Figure 2.5. In a binary image, if any pixels of neighboring pixels are zero, a pixel is set to zero. This operation removes the islands and little objects in the image. In brief, the morphological close operation is filling small gaps, and preserving the shape of the objects in the image is shown in Figure 2.6.

2.7 Hysteresis Thresholding

Hysteresis essentially comprises of deciding a high edge that enables a gathering of pixels to be delegated edge focuses without utilizing network data among them. A low edge at that point figures out which gathering of pixels won't be edge focuses and allows just those focuses that increase the availability of the recently decided edge focuses to be accumulated as edge focuses (Medina-Carnicer, Madrid-Cuevas, Carmona-Poyato, & Muñoz-Salinas, 2009).For instance, you may pick the high edge to be 0.8, this implies all pixels with an value bigger than 0.8 will be set to 1. You may likewise pick a low edge of 0.1, this implies all pixels short of what it's anything but an edge and you would set it to 0. The qualities in the middle of 0.1 and 0.8 would be weak edges.

Figure 2.6 Close operation performed image of sample image in Figure 1.1

2.8 Neural Network

Human brain contains neurons and each neuron is connected to another neuron. Some scientists think the brain is nonlinear, parallel computer and evidence proposes receive, analysis and transmit information. The information is transmitted in a form of electrochemical signals.

A neuron has a cell body, many signal inputs represented by dendrites and a single output named as axon. Neuron is connected to other neuron output that is axon through synapses, which is a very narrow gap. Figure 2.7, shows an illustration of basic model of a neuron. Here the neuron inputs are represented by x values, synapses are given as weight w, and the neuron output axon as y. It works in two stages – It computes the weighted total of its sources of information together with a threshold value and after that applies a linear of nonlinear function for output calculation. To generate a neuron to carry out a specific function, the neuron has to be trained. The weights of the neuron are trained in a way until the neuron becomes capable of making correct assumptions for the data which has not been used during the training. This process is called the generalization of the neuron or the network. Neuron connected in various ways is called as neural networks consisting of input layer, hidden layer and output layer. Figure 2.8 shows an illustration of a neural network.

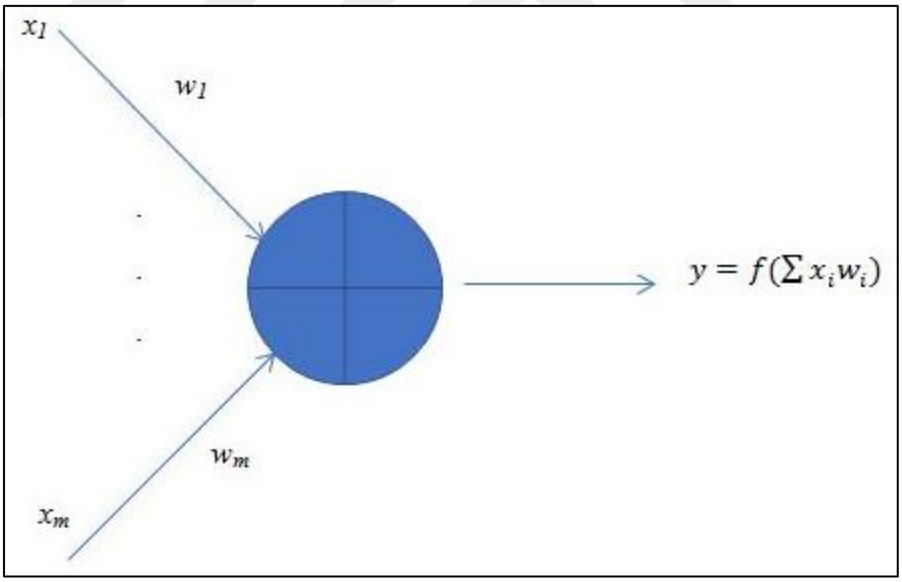

Figure 2.7 Integrated and fire neuron model

2.8.1 Input Layer of Neural Network

The principal layer of a neural system is input layer. It is utilized to give the information or highlights to the system. There is no calculation capability of this layer.

2.8.2 Output Layer of Neural Network

The output layer reports the estimations. The enactment capacity to be used in output layer is distinctive for various issues. For our algorithm, it is need to the yield to be either 0 or 1.

2.8.3 Hidden Layer of Neural Network

Hidden layer of a neural network provides connection between input layer and output layer. This layer is not seen from input and output, which is the reason to be called as hidden layer. The weights of hidden layer are trained to find the relation between the input and output. The weights of the layer represent different features of the trained data set.

For complex applications, the number of layer can be increased accordingly. In addition to number of layers, the number of neurons can also be different depending on the complexity of the transform. Generally, number of layers and number of neurons for each layer is found empirically. Increased number of neurons within the hidden layer may cause over fitting problem.

There are various types of neural networks and hidden layer may take different structures depending on the network type. At the output of hidden layer there is a function which gadders.

2.9 Feed Forward Neural Network

A Feed-forward Neural Network example which is most used in neural network applications is given in Figure 2.8. This network consists of three layers. They are input, output, and hidden layers. The number of hidden layer can change depending on the complexity of the job. The input layer has no computation neuron unit. Hidden layer and output layer neurons perform the calculations. This network is trained in supervised manner, for which input and output data available prior to the training. The network has to be tested with a data set that has not been seen during training to evaluate the capability of the network.

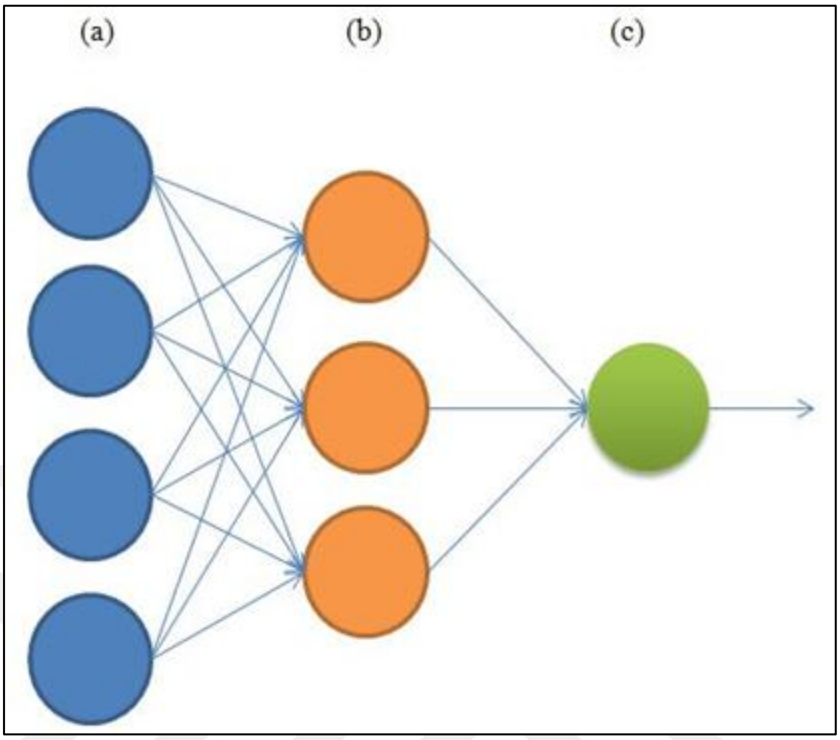

Figure 2.8 (a) is input, (b) hidden, and (c) output layers of neural-network

CHAPTER THREE
MULTIPLE FILTERING AND THRESHOLDING BASED CRACK DETECTION METHOD

We propose a novel crack detection method that consists of multiple filtering and hysteresis thresholding to decide whether an analyzed image has a crack or not. This proposed method is named as Multiple Filtering and Thresholding Based Crack Detection Method (FTCDM). This method gives a straightforward programmed crack discovery algorithm on pavement structures utilizing different sifting activities, numerous thresholding tasks, and morphological activities what's more; a few exact procedures are utilized to order cracks forms in the images.

3.1 Steps of the Hysteresis Crack Detection Method

The contribution of the recommended technique is a red-green-blue space image with 'jpg' expansion and developed in MATLAB R2016a programming. Nonetheless, the system could be effectively changed for some different augmentations. FTCDM is completed in the spatial area without utilizing preparing and color arrangement; along these lines it is quick and productive. The schematic of FTCDM is mentioned in Figure 3.1 and the stages of FTCDM can be sort as;

1. A sample image that is input from the image dataset.
2. The gray-scale format sample is acquired from the sample image in Figure 1.1.
3. To smooth out the surface, the Gaussian smoothing is enforced to the gray-scale image.
4. To remove the noise median filter is performed after Gaussian smoothing processing in Figure 2.1 to remove the noise.
5. To determine the Gradient magnitude and Gradient angle, the Median filtered image is utilized.
6. Non-maximum suppression (NMS) with using interpolation is performed.
7. Double-thresholding is performed after NMS processing.
8. Otsu's thresholding method is performed to double-thresholded image to get

the binary image.

9. The binary image is input for the Morphological technique.

10. The cracked and non-cracked image is determined with threshold method or neural network method.

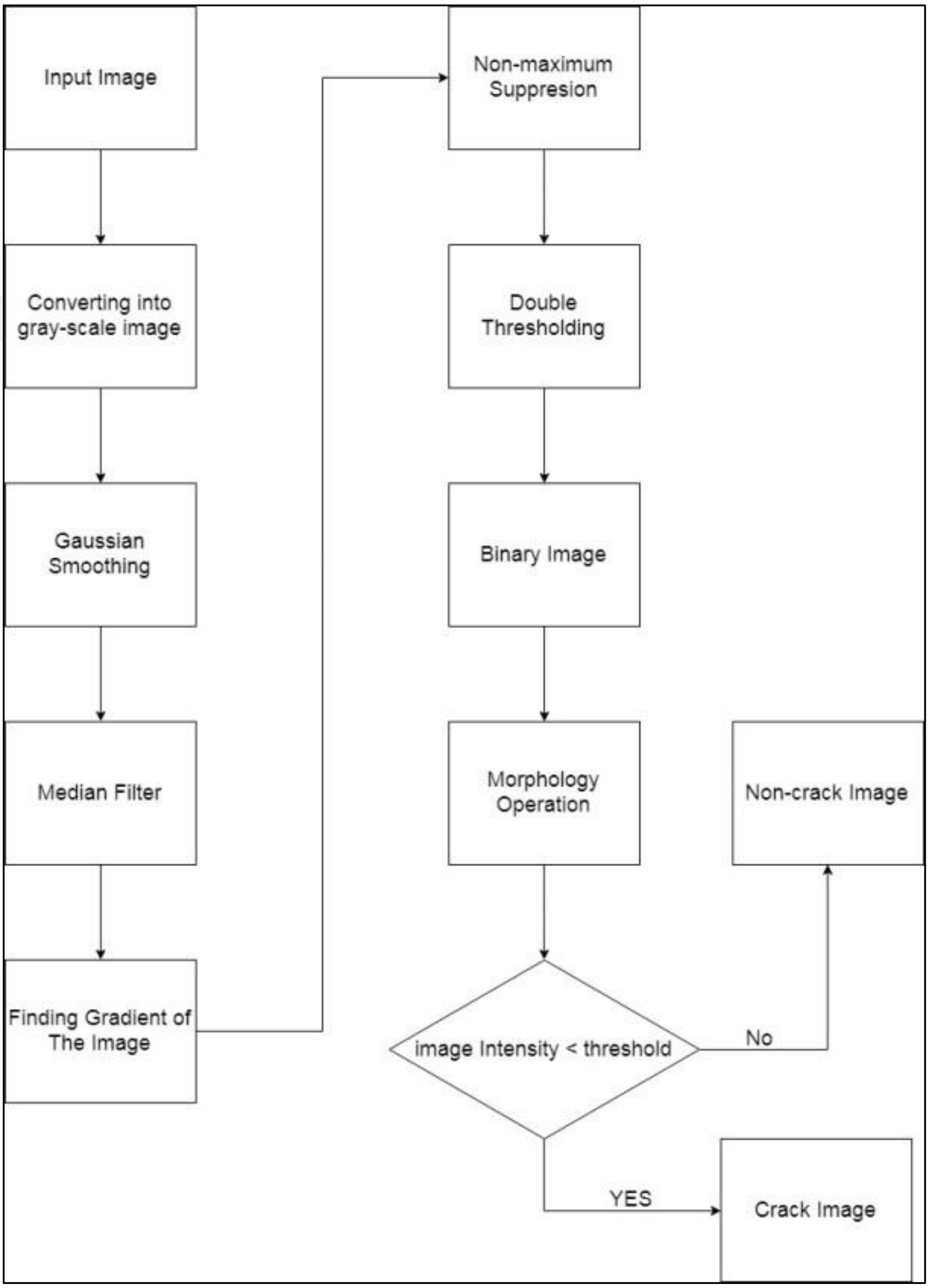

Figure 3.1 Flowchart of FTCDM

3.2 Explanation of the Hysteresis Crack Detection Method

The image dataset is taken from an open web source. In this dataset, the samples are taken from buildings at the Middle East Technical University campus. This dataset consists of 40000 images. The half of 40000 images is non-crack image samples; the other half is crack sample images (Ozgenel, 2018).

The initial step of FTCDM is to change over to the gray-scale image from the RGB image. Every pixel value of a RGB image takes part in 0 to 255. The transformation to gray-scale image is completed by equation 2.1. The gray-scale image of sample image in Figure 3.2 is shown in Figure 3.3.

To obtain blur images and remove noise from an image, Gaussian filtering is used by using two-dimensional Gaussian function given in equation 2.2. The Gaussian blurred image is shown in Figure 3.4.

Pavement surfaces are generally reliable with variations that are non-cracked from the norm. A Median filter in 5x5 is convoluted on the sample image to reduce noise. Entire image densities are interchanged with the matrix. It means that the center of the filter is set at a density that overlaps 25 pixels. After the median value of 25 pixels is determined and supplanted with the first force. For fringe intensities, densities with a value of zero, called zero padding, are defined. The Median filtered image is in the Figure 3.5.

The sudden change of image intensities compared to neighborhood pixels in a gray scale image shows the crack pixels in this image. So, the cracks on the image will be asserted with finding the gradient of the image. To find the edges on the image, Sobel operators are executed with the derivatives in horizontal and vertical direction are defined as in equation 2.3, equation 2.4.

After calculating gradient of the image that is shown in Figure 3.6, non-maximum suppression method is executed on this image and it is displayed in the Figure 3.7. The suppression of the local non-maxima of the magnitude of the gradient of image intensity in the direction of this gradient consists of four steps that are mentioned in section 2.5.

There can be noise in the gray-scale image and some edges may not be real edges. Hysteresis thresholding helps to remove the noise. In the double thresholding method, there are two threshold values they are high threshold value and low threshold value, and indicated as (t_h) and (t_l), respectively. Using these threshold values, pixel values will be set or clear. The pixel value is set, if this value is greater than t_h, When the pixel value is lower than t_l, the pixel value is clear. These threshold values (t_h and t_l) are calculated experimentally. The result of hysteresis thresholding is demonstrated in Figure 3.8.

A global threshold is computed with using Otsu's threshold method (Otsu, 1979). The Otsu method selects a threshold that limits the intraclass variance of the high contrast pixels with threshold. The global threshold can be utilized with MATLAB imbinarize function to change over a gray-scale image into a binary image (*BW*) in Figure 3.9.

After the Otsu's threshold method is executed, the morphological close operation is applied to the black-white image to join two near pixels of the *BW* image and then the final image is obtained in Figure 3.10.

At the end of eight stages, the method generates an image consisting of binary values. The method calculates similar images for every image in dataset. (Abdel-Qader et. al., 2003) proposes a threshold value t_c, which is average value of the all pixels in the entire image dataset. In this research, a threshold value t_c is calculated in the same manner. At the nineth stage of FTCDM, binary images of all crack and non-crack images are generated. Then a threshold value is calculated as described above for all generated images. Again at the same stage, if the intensity of the final image of the sample image is less than t_c, this sample image is determined as non-cracked image. Unlike this situation, if the intensity of the final image of the sample image is greater than t_c, the sample image is determined as cracked image.

The final images of the sample images are input of the FTCDM with using neural network, which have one input layer, one hidden layer, and one output layer. The target matrix of the neural network is calculated for cracked sample images and non-cracked sample images. When the input matrix of neural network is cracked image sample, the output matrix value is 1. The output matrix value is 0 when the input matrix of neural network is non-cracked image sample. Using the output and input matrices feed forward neural network is trained. The test image that is not part of input of the neural network is determined as cracked or non-cracked image with using neural network.

Figure 3.2 The crack sample image #2 (Ozgenel, 2018)

Figure 3.3 The gray level form of Figure 3.2

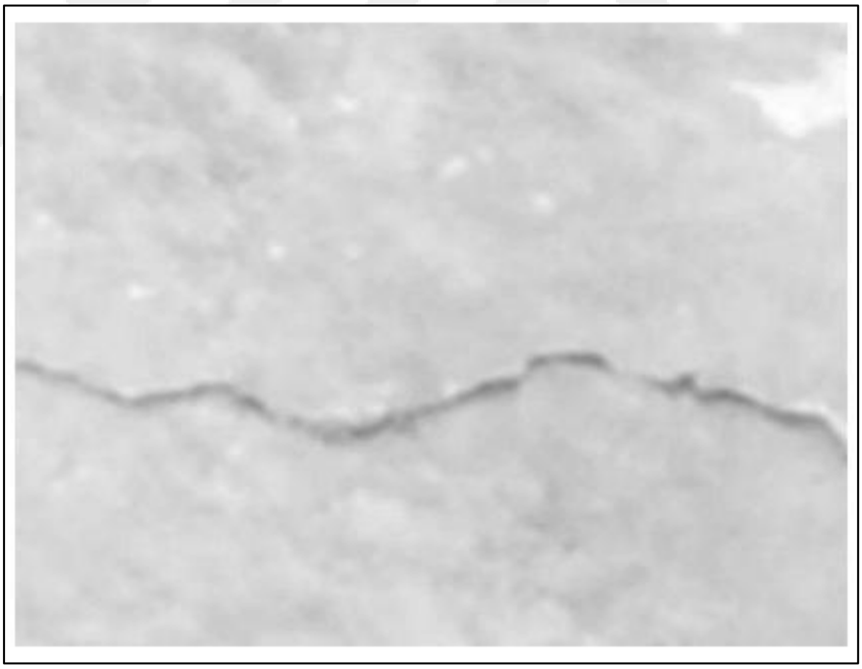

Figure 3.4 The Gaussian blurred image of Figure 3.3

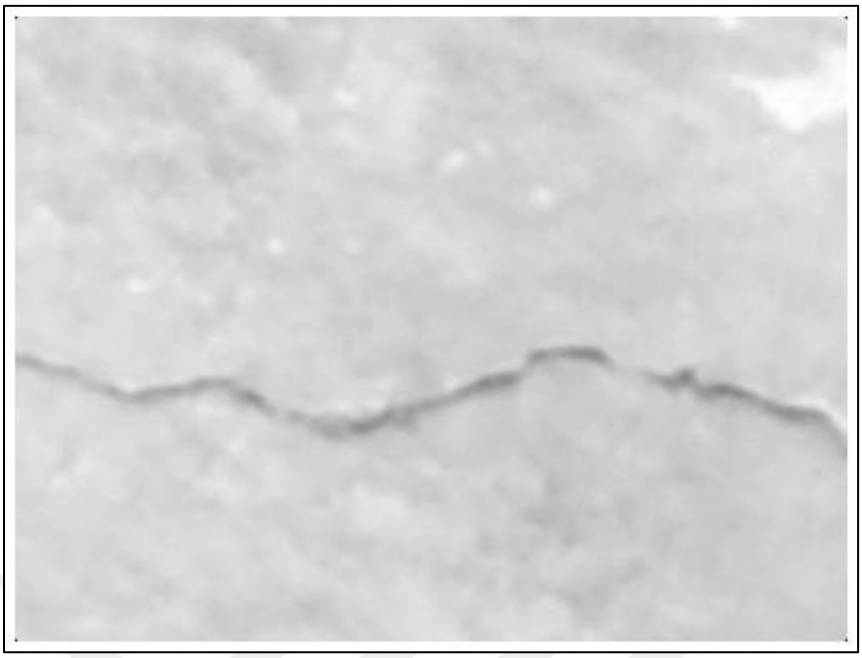

Figure 3.5 The Median filtered image of Figure 3.4

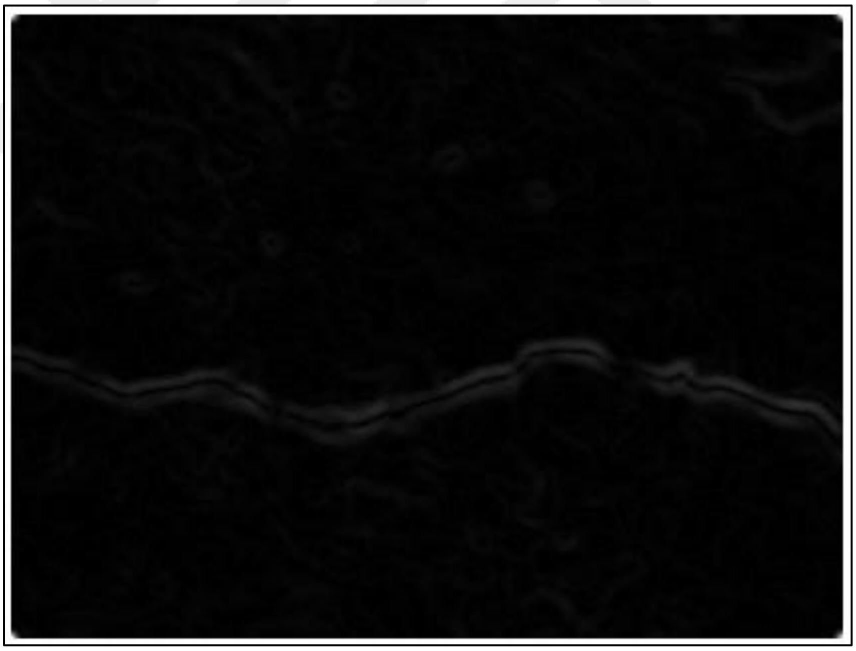

Figure 3.6 The gradient image of Figure 3.5

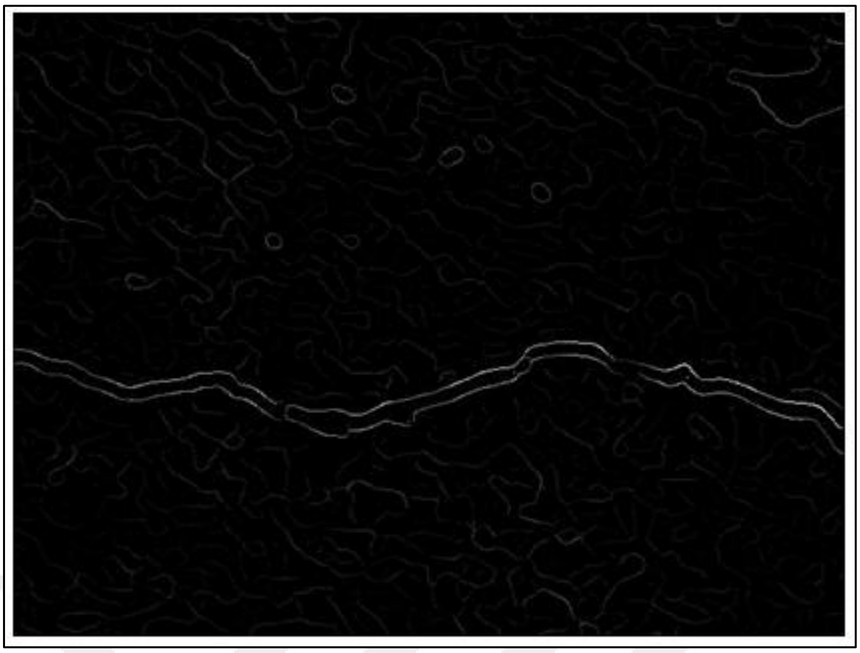

Figure 3.7 The image performed NMS of Figure 3.6

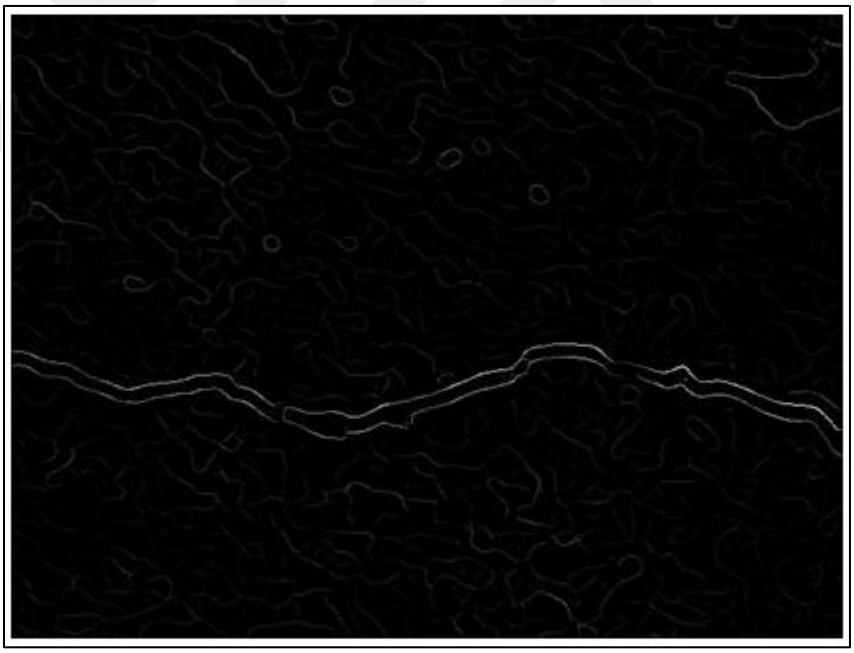

Figure 3.8 The double-thresholded image of Figure 3.7

Figure 3.9 The binary form of Figure 3.8

Figure 3.10 The Morphological operated image of Figure 3.9

CHAPTER FOUR
EXPERIMENTAL RESULTS AND DISCUSSIONS

The image is determined as cracked or non-cracked image by using determined crack threshold value t_c which is mentioned in section 3.2. When FTCDM is performed on 100 non-cracked images, the result is shown in Figure 4.1. The determination of the non-crack image is mentioned in section 3.2. As seen from Figure 4.1, four image intensities are below the determined crack threshold value. Therefore, these images will be accepted as crack images. In this case, the correct prediction percentage of non-crack detection determined by the FTCDM is 96 out of 100 images. The accuracy of FTCDM for non-crack sample images is equal to 96%.

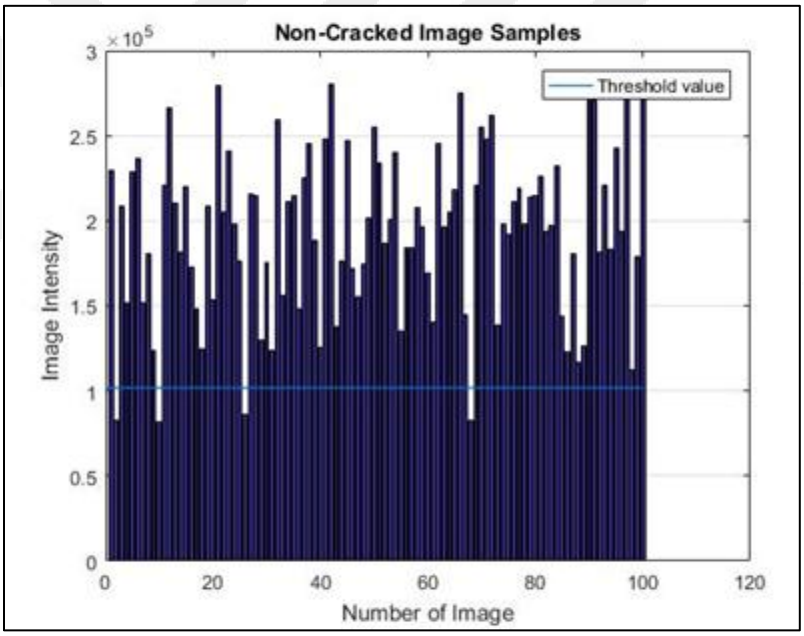

Figure 4.1 Image intensities of non-cracked samples for FTCDM

When FTCDM is run over on the 100 cracked sample images from the dataset, the result of FTCDM of 100 sample images is shown in Figure 4.2. A sample image is determined as crack image, when the intensity value of the image is lower than the crack threshold value t_c. When the results are examined it can easily be seen that except one, all other 99 sample image intensities are lower than the t_c value. It means the number of correct crack detections percentage performed by this method is 99 out of 100 images. The total accuracy of this method for crack sample images is equal to

99%. The overall accuracy of FTCDM for two-hundred image dataset is equal to 97.5%.

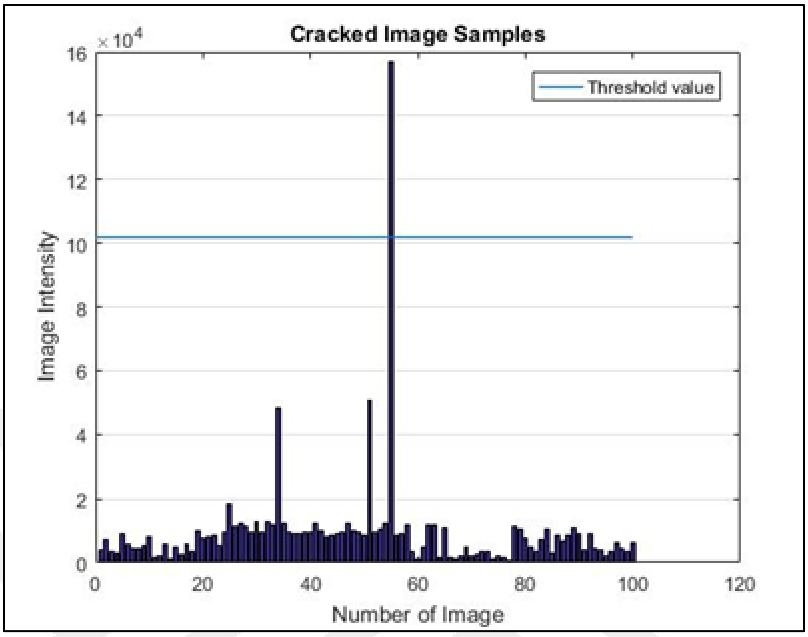

Figure 4.2 Image intensities of cracked samples for FTCDM

It can be seen from Figure 4.1 and Figure 4.2, average of non-crack image intensities is higher than average of crack image intensities. The reason for this is morphological operation, which fills the gap between the near pixels that is one. This clearly increases the image intensity.

The crack detection accuracy rates of FTCDM are mentioned in Table 4.1. FTCDM provides 99% successes rate of true positive and 96% true negative. The TP rate of Abdel-Qader's method is equal to 96% and the false negative rate of the Abdel-Qader's method is 76% (Abdel-Qader et. al., 2003). Two application use different dataset.

The dataset for system performance analysis consists of 200 images, 50% of which is cracked and the other half is non-cracked image intensities. FTCDM with a neural network classifier is trained with 80 crack and 80 non-crack sample image intensities. The remaining 20% of the complete dataset is used to test the generalization capability of the neural network. The test image intensity dataset included 20 crack samples and 20 non-crack samples.

Table 4.1 Crack detection accuracy for FTCDM and FTCDM with neural network

Method	True Positive	True Negative	False Positive	False Negative
FTCDM	99%	96%	4%	1%
FTCDM with neural network	100%	0%	0%	100%

The stages of the FTCDM that is for crack samples are shown in Figure 4.3, Figure 4.4, Figure 4.5, Figure 4.6, Figure 4.7, Figure 4.8, Figure 4.9, Figure 4.10, Figure 4.11, and Figure 4.12. In these figures, there are nine stages of proposed method. Stage 1 corresponds to original image, stage 2 corresponds to gray-scale image of stage 1, stage 3 corresponds to Gaussian filtered image of stage 2, stage 4 corresponds to corresponds to Median filtered image of stage 3, stage 5 corresponds to gradient image of stage 4, stage 6 corresponds to non-maximum suppressed image of stage 5, stage 7 corresponds to double-thresholded image of stage 6, stage 8 is binary image of stage 7, and the last stage 9 is morphological operated image of stage 8.

The steps of the FTCDM that is mentioned in section 3.1 for non-crack samples is shown in Figure 4.13, Figure 4.14, Figure 4.15, Figure 4.16, Figure 4.17, Figure 4.18, Figure 4.19, Figure 4.20, Figure 4.21, and Figure 4.21. The stages, which are shown in these figures, are same with stages in Figure 4.3.

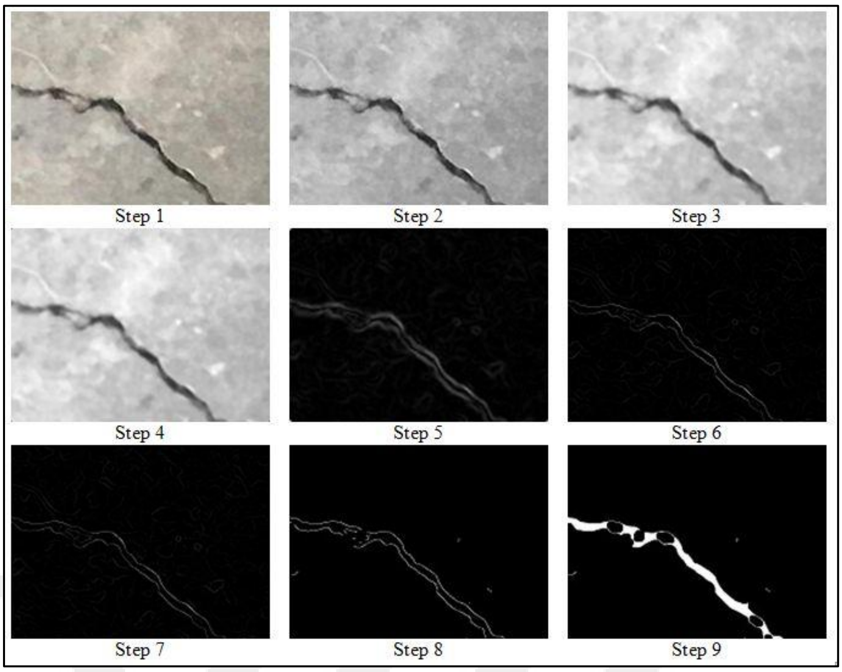

Figure 4.3 These are the stages for FTCDM on the crack sample #1

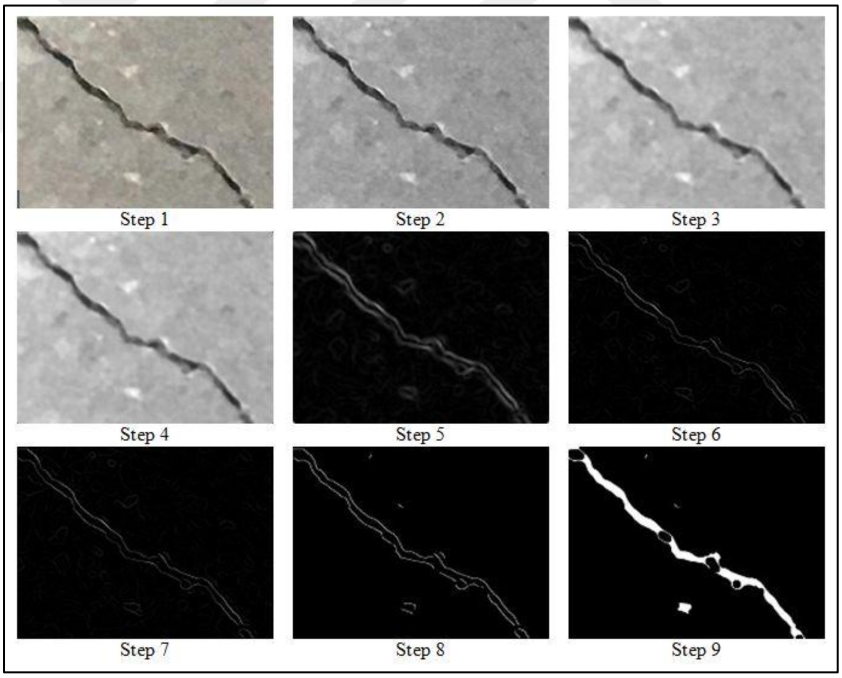

Figure 4.4 These are the steps for FTCDM on the crack sample #2

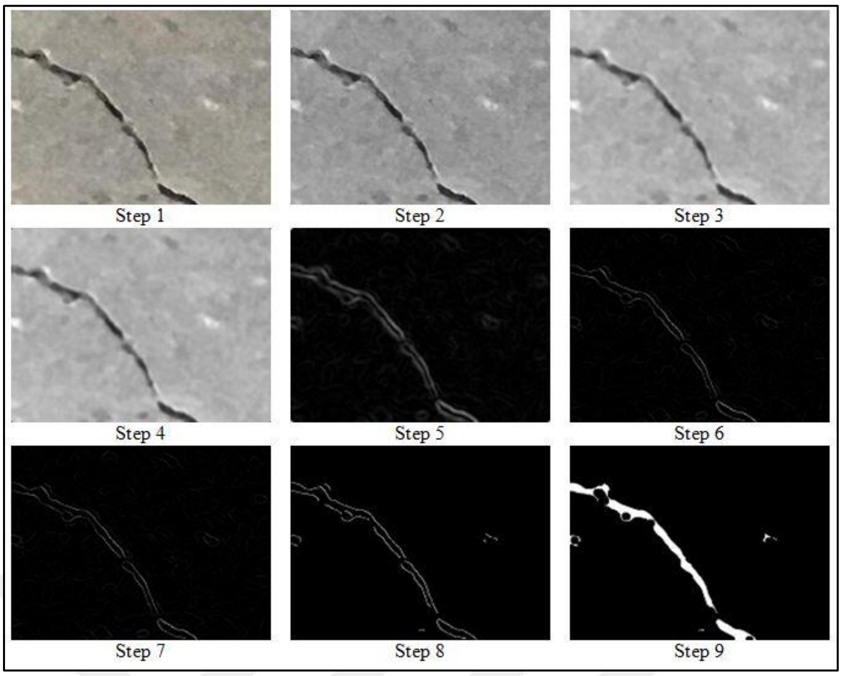

Figure 4.5 These are the steps for FTCDM on the crack sample #3

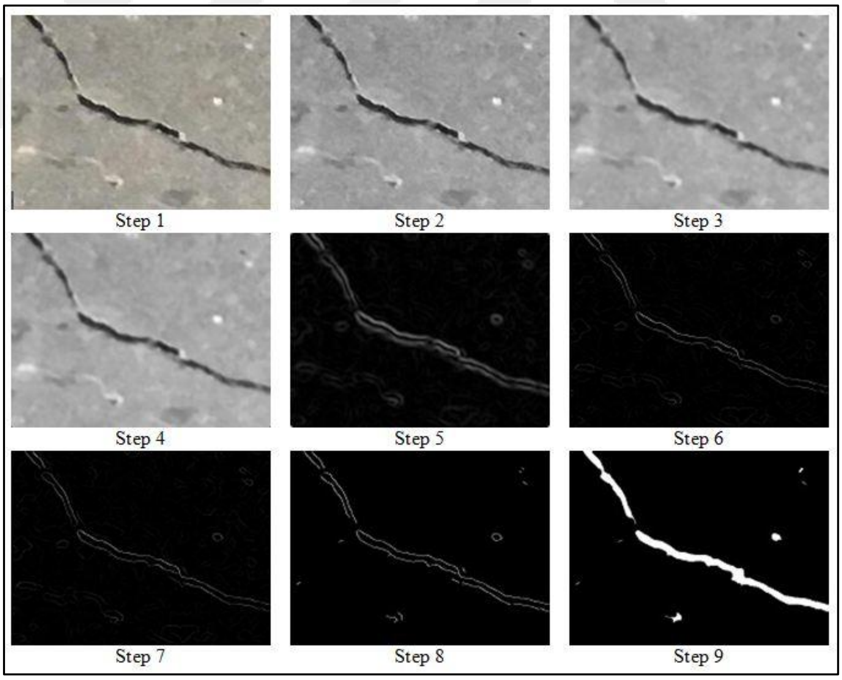

Figure 4.6 These are the steps for FTCDM on the crack sample #4

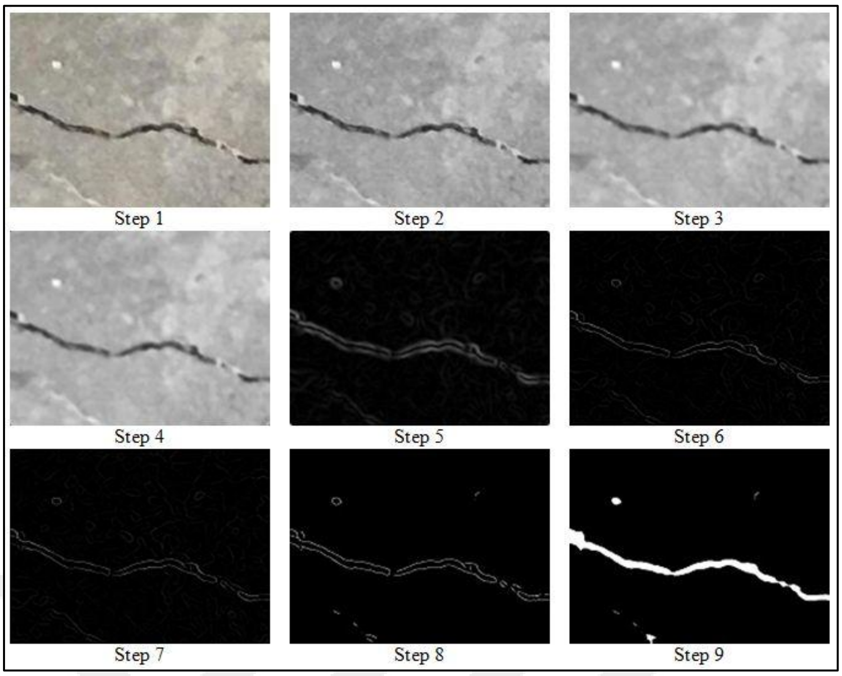

Figure 4.7 These are the steps for FTCDM on the crack sample #5

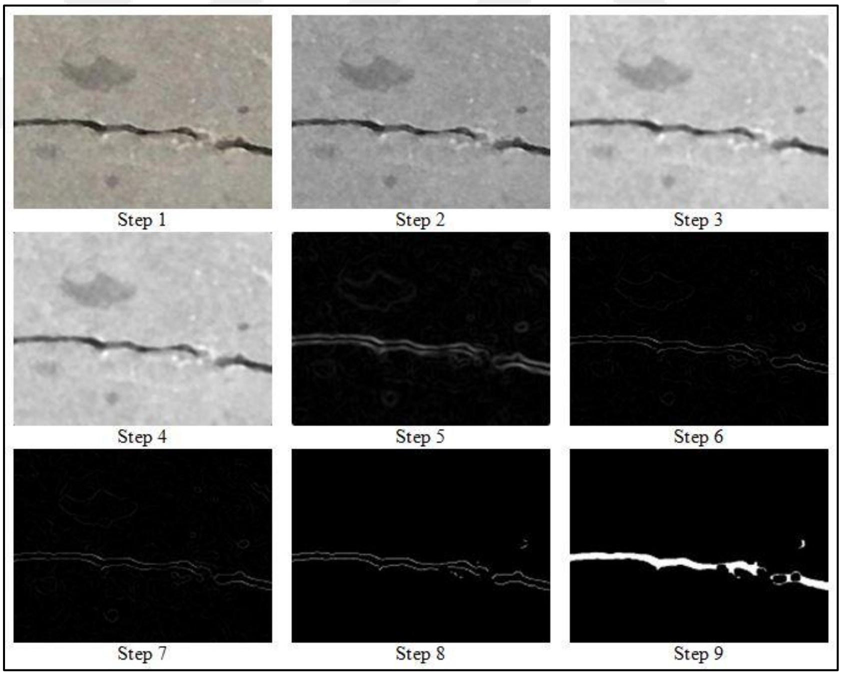

Figure 4.8 These are the steps for FTCDM on the crack sample #6

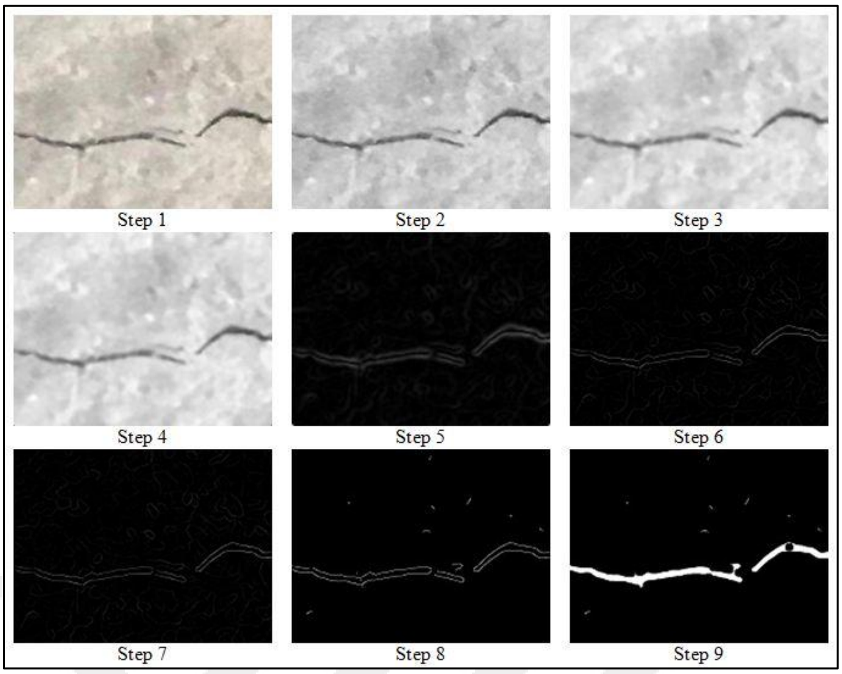

Figure 4.9 These are the steps for FTCDM on the crack sample #7

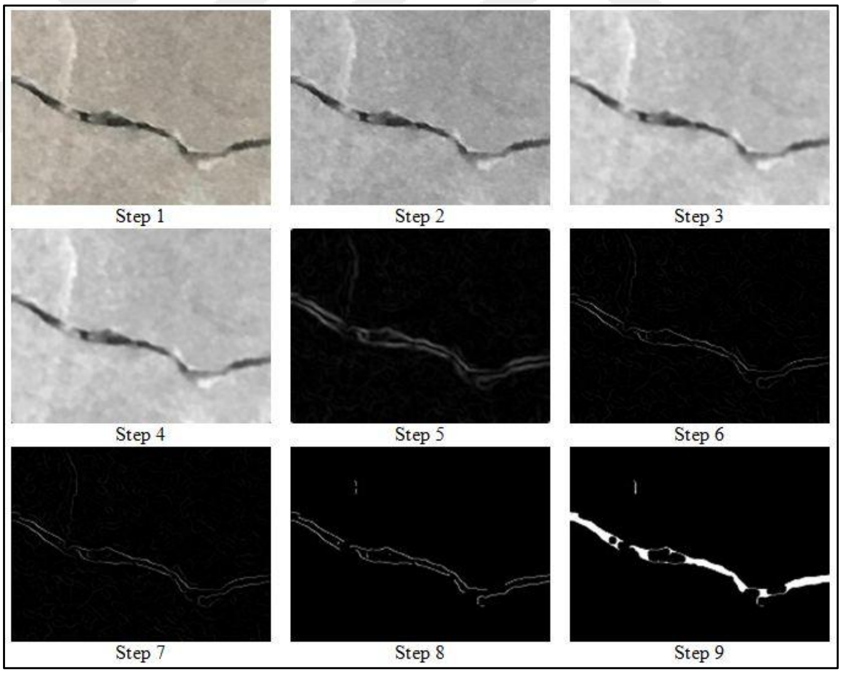

Figure 4.10 These are the steps for FTCDM on the crack sample #8

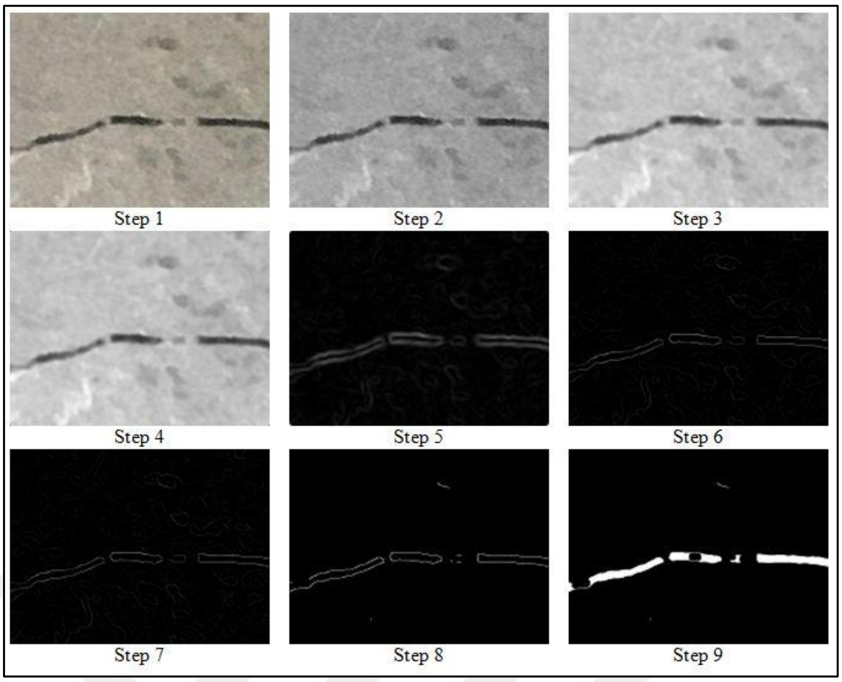

Figure 4.11 These are the steps for FTCDM on the crack sample #9

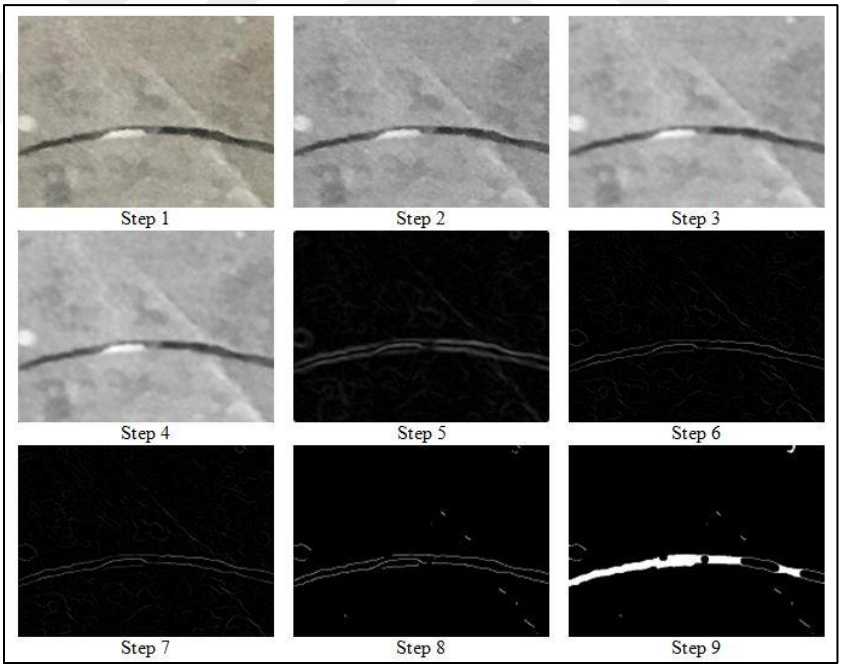

Figure 4.12 These are the steps for FTCDM on the crack sample #10

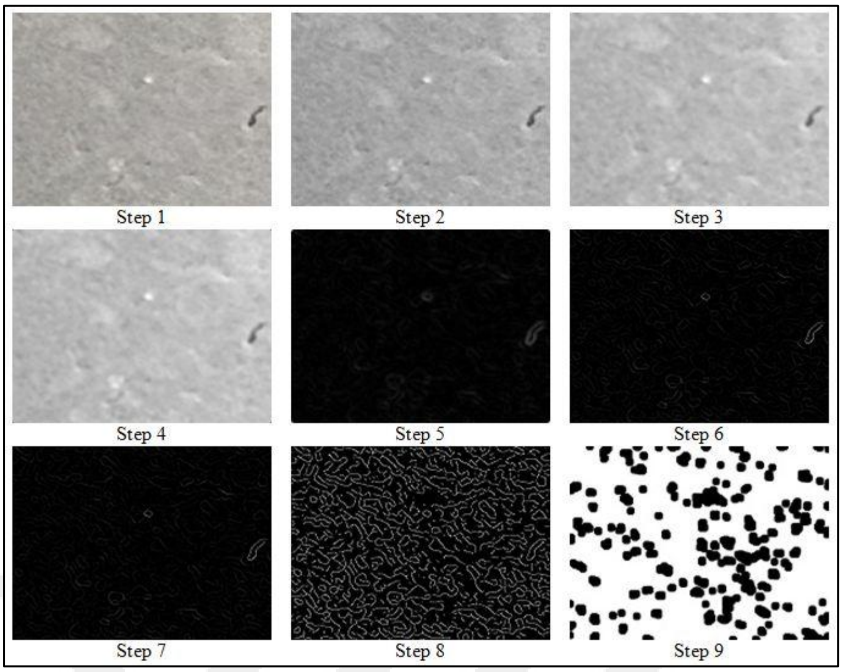

Figure 4.13 These are the steps for FTCDM on the non-crack sample #1

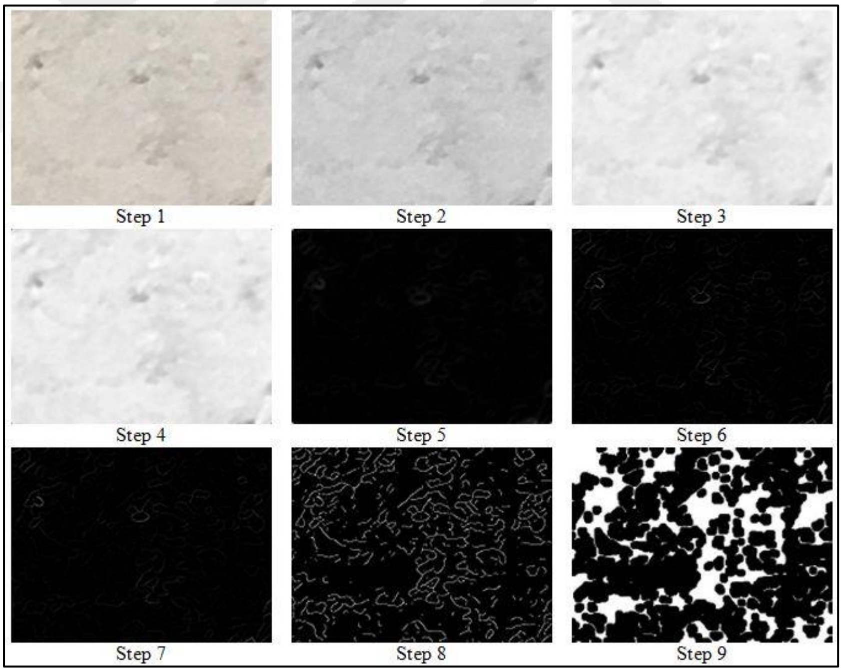

Figure 4.14 These are the steps for FTCDM on the non-crack sample #2

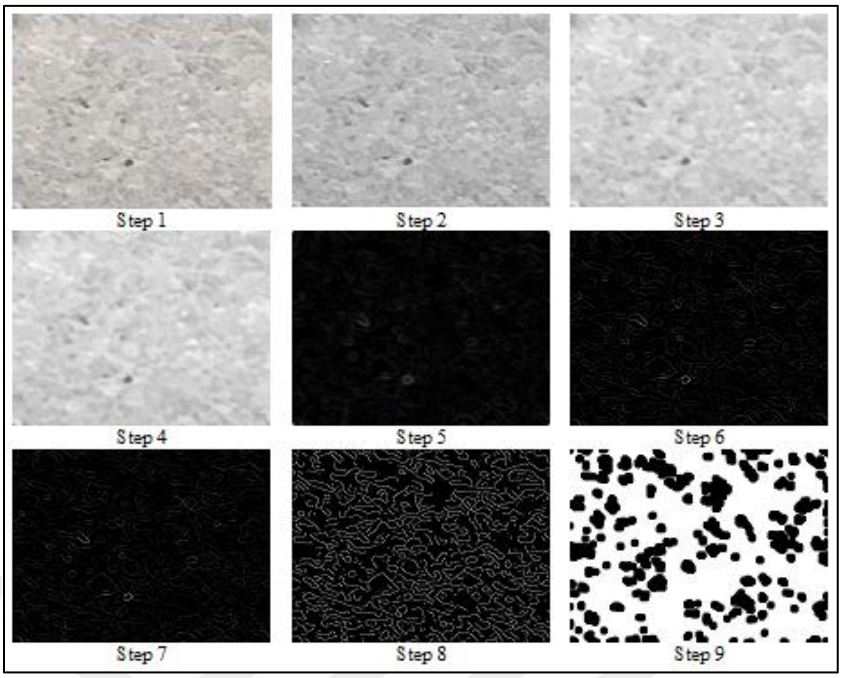

Figure 4.15 These are the steps for FTCDM on the non-crack sample #3

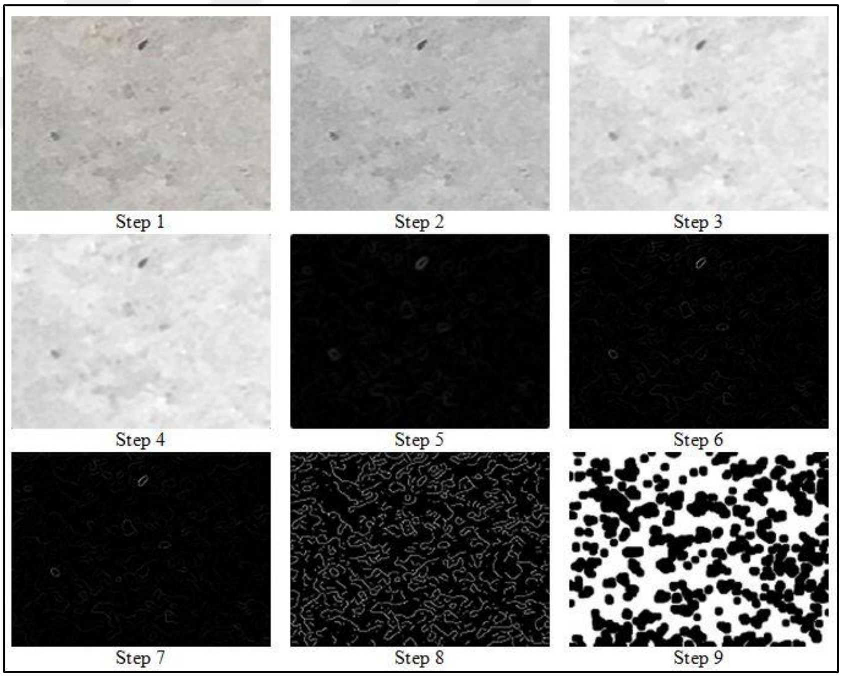

Figure 4.16 These are the steps for FTCDM on the non-crack sample #4

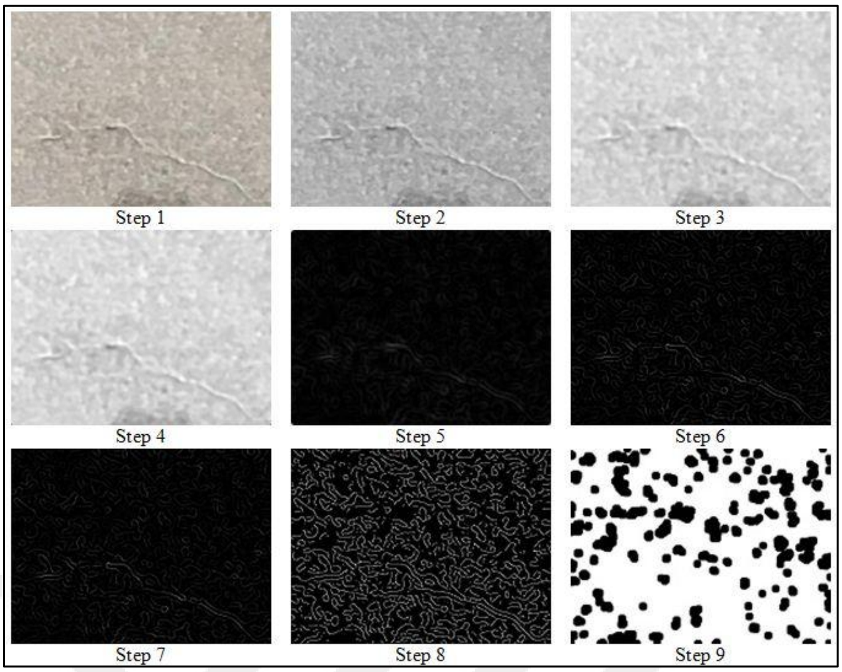

Figure 4.17 These are the steps for FTCDM on the non-crack sample #5

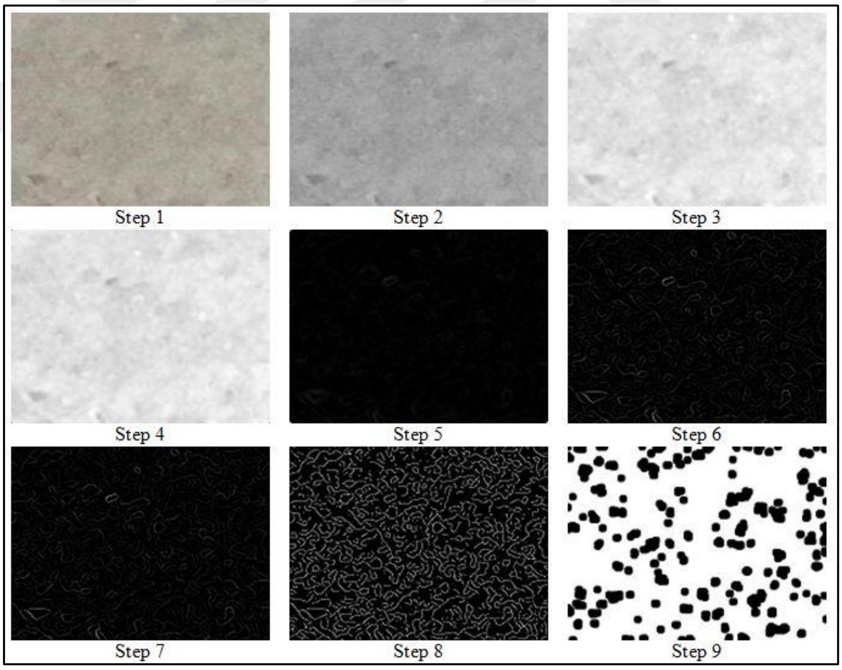

Figure 4.18 These are the steps for FTCDM on the non-crack sample #6

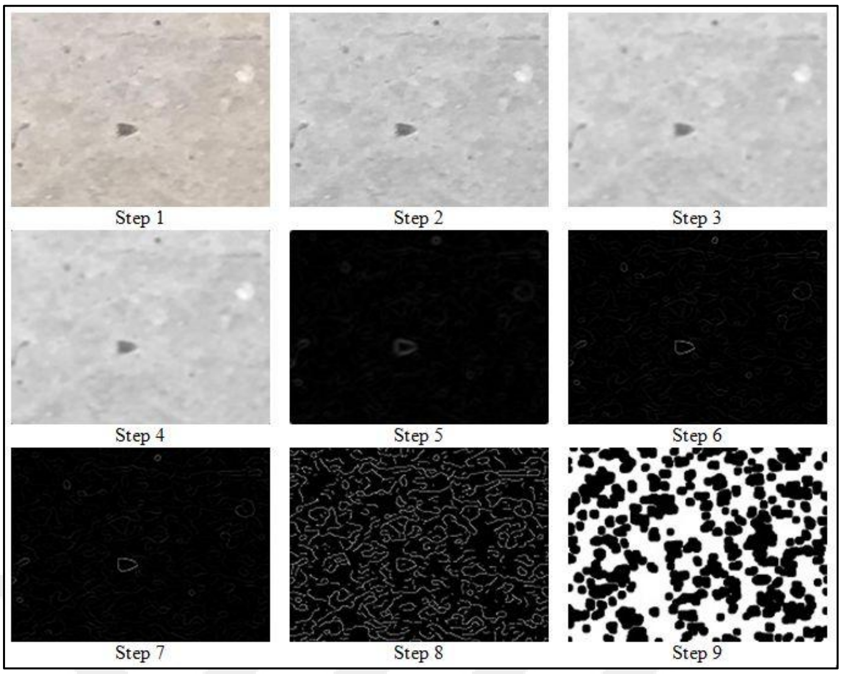

Figure 4.19 These are the steps for FTCDM on the non-crack sample #7

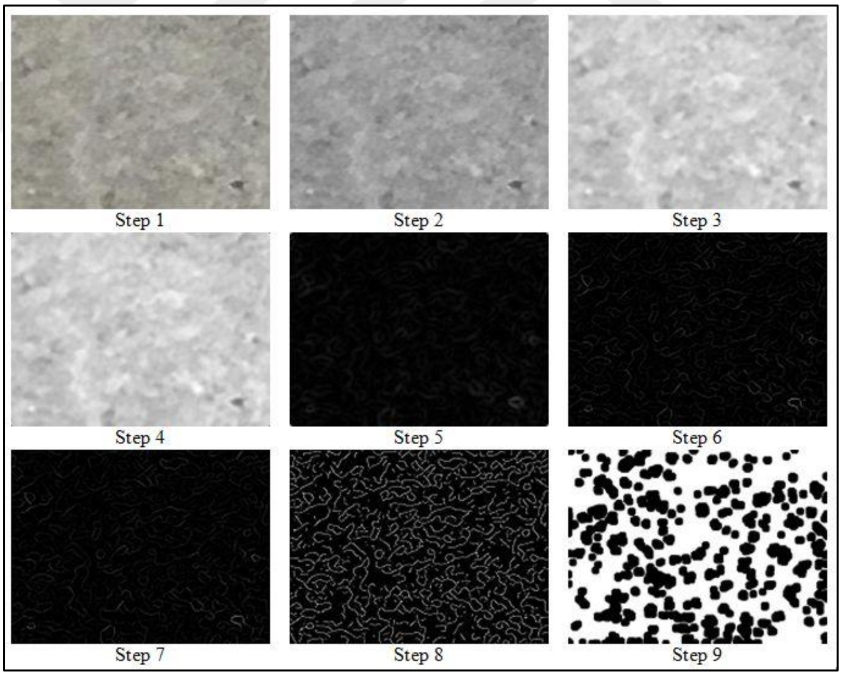

Figure 4.20 These are the steps for FTCDM on the non-crack sample #8

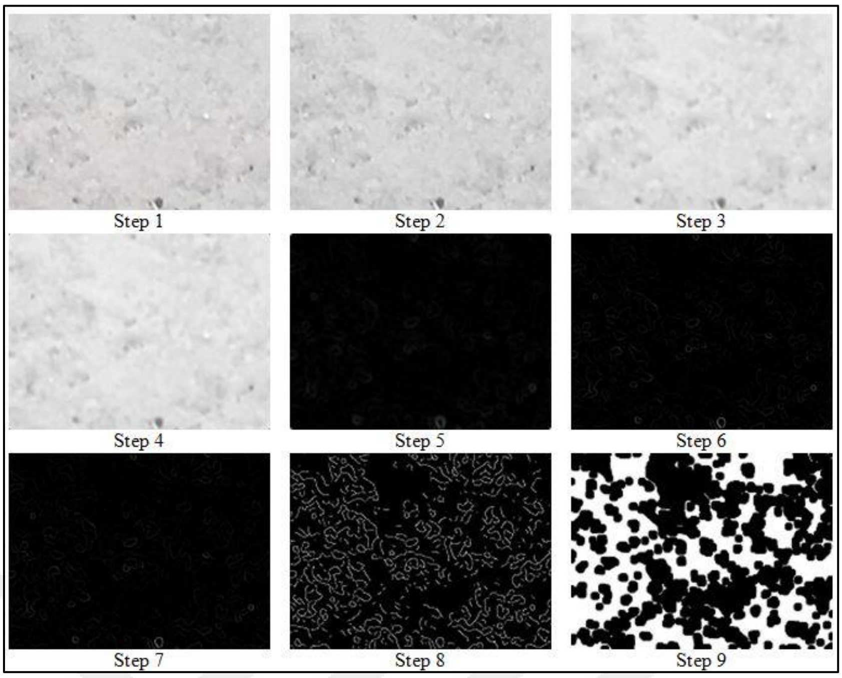

Figure 4.21 These are the steps for FTCDM on the non-crack sample #9

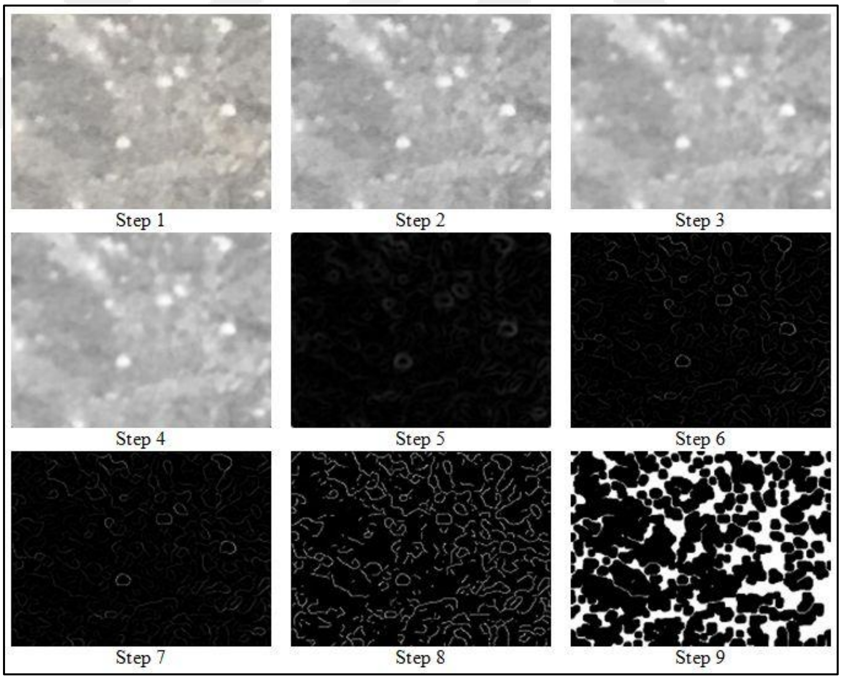

Figure 4.22 These are the steps for FTCDM on the non-crack sample #10

CHAPTER FIVE
CONCLUSION

In this thesis the crack detection system is implemented on the crack and non-crack sample images to avoid destruction of the structures. Multiple filtering and thresholding based crack detection method (FTCDM) is proposed for surface crack detection in concrete structures.

The FTCDM is a hybrid method and consists of nine processing stages; obtaining gray scale format image from sample image, smoothing the structure with using Gaussian filter and Median Filter, determining gradient magnitude and angle, performing non-maximum suppressing, double-thresholding, image binarization, performing morphological operations and finally determining the image is crack or non-cracked with using crack threshold value that is mentioned in section 3.2, respectively. At the end of nine stages the method determines the intensity of all images in binary format and generates a threshold value t_c. Depending on the threshold value, the method decides whether the sample image is crack image or non-crack image. The accuracies of FTCDM are 96% and 99% for non-crack images and crack-images, respectively. The total accuracy of FTCDM for two-hundred image dataset is equal to 97.5%.

To increase the accuracy of the proposed method, a neural network is added to system. The neural network is a feed-forward type and has a single hidden layer. The network was trained with 80 non-crack image intensities and 80 crack image intensities. Finally, the neural network was tested with total of 40 sample image intensities in which half of it crack images and the other half is non-crack images. The total accuracy of FTCDM with neural network for two-hundred image dataset is equal to 100%.

FTCDM has been implemented with dataset provided by (Ozgenel, 2018). However, as a future work this method has to be compared with other techniques on the same dataset to evaluate the success.

REFERENCES

Abdel-Qader, I., Abudayyeh, O., & Kelly, M. (2003). Analysis of edge-detection techniques for crack identification in bridges. *Journal of Computing in Civil Engineering*, *17*(4), 255-263.

Akagic, A., Buza, E., Omanovic, S., & Karabegovic, A. (2018). Pavement crack detection using otsu thresholding for image segmentation. *2018 41st International Convention on Information and Communication Technology, Electronics and Microelectronics, MIPRO 2018 - Proceedings*, 1092-1097.

Amhaz, R., Chambon, S., Idier, J., & Baltazart, V. (2014). A new minimal path selection algorithm for automatic crack detection on pavement images. *2014 IEEE International Conference on Image Processing (ICIP)*, 788-792.

Choudhary, G., & Dey, S. (2012). Crack detection in concrete surfaces using image processing, fuzzy logic, and neural networks. *2012 IEEE Fifth International Conference on Advanced Computational Intelligence (ICACI)*, 404-411.

Giakoumis, I., Nikolaidis, N., & Pitas, I. (2006). Digital image processing techniques for the detection and removal of cracks in digitized paintings. *IEEE Transactions on Image Processing*, *15*(1), 178-188.

Hu, D., Tian, T., Yang, H., Xu, S., & Wang, X. (2012). Wall crack detection based on image processing. *2012 Third International Conference on Intelligent Control and Information Processing*, 597-600.

Huayong Wu, Rongxin Zhao, & Bo Li. (2011). Crack image processing using probability based threshold. *2011 International Conference on Multimedia Technology*, 3904-3907.

Li, J., & Wang, N. (2015). A study of crack detection algorithm. *2015 Fifth International Conference on Instrumentation and Measurement, Computer, Communication and Control (IMCCC)*, 1184-1187.

Lins, R., & Givigi, S. (2016). Automatic crack detection and measurement based on image analysis. *IEEE Transactions on Instrumentation and Measurement*, *65*(3), 583-590.

Mancini, A., Malinverni, E., Frontoni, E., & Zingaretti, P. (2013). Road pavement crack automatic detection by MMS images. *21st Mediterranean Conference on Control and Automation*, 1589-1596.

Maode, Y., Shaobo, B., Kun, X., & Yuyao, H. (2007). Pavement crack detection and analysis for high-grade highway. *2007 8th International Conference on Electronic Measurement and Instruments*, 548-552.

Medina, R., Llamas, J., Zalama, E., & Gomez-Garcia-Bermejo, J. (2014). Enhanced automatic detection of road surface cracks by combining 2d/3d image processing techniques. *2014 IEEE International Conference on Image Processing (ICIP)*, 778-782.

Medina-Carnicer, R., Madrid-Cuevas, F., Carmona-Poyato, A., & Muñoz-Salinas, R. (2009). On candidates selection for hysteresis thresholds in edge detection. *Pattern Recognition, 42*(7), 1284-1296.

Nishikawa, T., Yoshida, J., Sugiyama, T., & Fujino, Y. (2012). Concrete crack detection by multiple sequential image filtering. *Computer-Aided Civil and Infrastructure Engineering, 27*(1), 29-47.

Oliveira, H., & Correia, P. (2014). CrackIT - An image processing toolbox for crack detection and characterization. *2014 IEEE International Conference on Image Processing (ICIP)*, 798-802.

Oliveira, H., & Correia, P. (2017). Road surface crack detection: improved segmentation with pixel-based refinement. *2017 25th European Signal Processing Conference (EUSIPCO)*, 2026-2030.

Oliveira, H., & Lobato Correia, P. (2008). Identifying and retrieving distress images from road pavement surveys. *2008 15th IEEE International Conference on Image Processing*, 57-60.

Otsu, N. (1979). A threshold selection method from gray-level histograms. *IEEE Transactions on Systems, Man, and Cybernetics*, *9*(1), 62-66.

Ozgenel, C.F., (2018, January 15). *Concrete crack images for classification*. Retrieved September, 15, 2018, from https://data.mendeley.com/datasets/5y9wdsg2zt/1

Premachandra, C., Waruna, H., Premachandra, H., & Parape, C. (2013). Image based automatic road surface crack detection for achieving smooth driving on deformed roads. *2013 IEEE International Conference on Systems, Man, and Cybernetics*, 4018-4023.

Qi, D., Liu, Y., Wu, X., & Zhang, Z. (2014). An algorithm to detect the crack in the tunnel based on the image processing. *2014 Tenth International Conference on Intelligent Information Hiding and Multimedia Signal Processing*, 860-863.

Qiang, S., Guoying, L., Jingqi, M., & Hongmei, Z. (2016). An edge-detection method based on adaptive canny algorithm and iterative segmentation threshold. *2016 2nd International Conference on Control Science and Systems Engineering (ICCSSE)*, 64-67.

Qingbo, Z. (2016). Pavement crack detection algorithm based on image processing analysis. *2016 8th International Conference on Intelligent Human-Machine Systems and Cybernetics (IHMSC)*, *1*, 15-18.

Rothe R., Guillaumin M., & Van Gool L. (2015) Non-maximum suppression for object detection by passing messages metween windows. in: Cremers D., Reid I., Saito H., Yang MH. (eds) Computer Vision -- ACCV 2014. ACCV 2014. *Lecture Notes in Computer Science, 9003*, (290-306) Cham: Springer.

Shen, G. (2016). Road crack detection based on video image processing. *2016 3rd International Conference on Systems and Informatics (ICSAI)*, 912-917.

Subirats, P., Dumoulin, J., Legeay, V., & Barba, D. (2006). Automation of pavement surface crack detection using the continuous wavelet transform. *2006 International Conference on Image Processing*, 3037-3040.

Sy, N., Avila, M., Begot, S., & Bardet, J. (2008). Detection of defects in road surface by a vision system. *MELECON 2008 - The 14th IEEE Mediterranean Electrotechnical Conference*, 847-851.

Talab, A., Huang, Z., Xi, F., & HaiMing, L. (2016). Detection crack in image using Otsu method and multiple filtering in image processing techniques. *Optik, 127*(3), 1030-1033.

Wang, P., & Huang, H. (2010). Comparison analysis on present image-based crack detection methods in concrete structures. *2010 3rd International Congress on Image and Signal Processing*, 5, 2530-2533.

Xu, G., Ma, J., Liu, F., & Niu, X. (2008). Automatic recognition of pavement surface crack based on bp neural network. *2008 International Conference on Computer and Electrical Engineering*, 19-22.

Xuhang Tong, Jie Guo, Yun Ling, & Zhouping Yin. (2011). A new image-based method for concrete bridge bottom crack detection. *2011 International Conference on Image Analysis and Signal Processing*, 568-571.

Yang, Y.-S., Yang, C.-M., & Huang, C.-W. (2015). Thin crack observation in a reinforced concrete bridge pier test using image processing and analysis. *Advances in Engineering Software, 83*, 99-108.

Zhang, L., Yang, F., Daniel Zhang, Y., & Zhu, Y. (2016). Road crack detection using deep convolutional neural network. *2016 IEEE International Conference on Image Processing (ICIP)*, 3708-3712.

Zhaoyun, S., Chaofan, W., & Aimin, S. (2009). Study of image-based pavement cracking measurement techniques. *2009 9th International Conference on Electronic Measurement & Instruments*, 140-143.